Introducing bioflocculation boundaries in process control to enhance effluent quality of high-rate contact-stabilization systems

Introducing Bioflocculation Boundaries in Process Control to Enhance Effluent Quality of High-Rate Contact-Stabilization Systems

Khoa Nam Ngo[1,2**], Patrexia Tampon[1,2*], Tim Van Winckel[3], Arash Massoudieh[2], Belinda Sturm[4], Charles Bott[5], Bernhard Wett[6], Sudhir Murthy[7], Siegfried E. Vlaeminck[3], Christine DeBarbadillo[1] and Haydée De Clippeleir[1]

[1]*District of Columbia Water and Sewer Authority, Blue Plains Advanced Wastewater Treatment Plant, Washington DC, USA*

[2]*Department of Civil and Environmental Engineering, The Catholic University of America, Washington DC, USA*

[3]*Research Group of Sustainable Energy, Air and Water Technology, Department of Bioscience Engineering, University of Antwerp, Belgium*

[4]*Department of Civil, Environmental and Architectural engineering, The University of Kansas, KS, USA*

[5]*Hampton Roads Sanitation District, VA, USA*

[6]*ARA consult GmbH, Austria*

[7]*NEWhub Corp., Herndon, Virginia, USA*

Email: 12ngo@cua.edu

*Equally contributing first author

**Corresponding author: Ngo, Khoa Nam

Abstract

High-rate activated sludge (HRAS) systems suffer from high variability of effluent quality, clarifier performance, and carbon capture. This study proposed a novel control approach using bioflocculation boundaries for wasting control strategy to enhance effluent quality and stability while still meeting carbon capture goals. The bioflocculation boundaries were developed based on the oxygen uptake rate (OUR) ratio between contactor and stabilizer (feast/famine) in a high-rate contact stabilization (CS) system and this OUR ratio was used to manipulate the wasting setpoint. Increased oxidation of carbon or decreased wasting was applied when OUR ratio was <0.52 or >0.95 to overcome bioflocculation limitation and maintain effluent quality. When no bioflocculation limitations (OUR ratio within 0.52 – 0.95) were detected carbon capture was maximized. The proposed control concept was shown for a fully automated OUR-based control system as well as for a simplified version based on direct waste flow control. For both cases, significant improvements in effluent suspended solids level and stability (<50 mg TSS/L), solids capture over the clarifier (>90%), and COD capture (median of 32%) were achieved. This study shows how one can overcome the process instability of current HRAS systems and provide a path to achieve more reliable outcomes.

Key words: High-rate activated sludge, Settleability, Clarifier performance, A/B process, Energy recovery

Abstract Graph

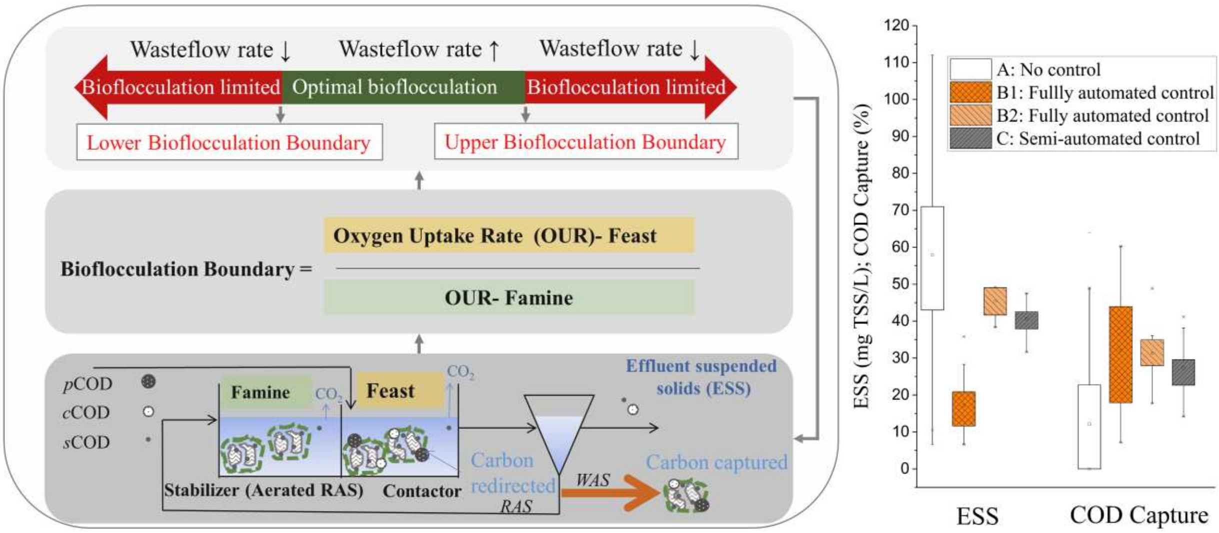

Practitioner points:

- Online bioflocculation boundaries (upper and lower limit) were defined by the OUR ratio between contactor and stabilizer (feast/famine).
- To maintain effluent quality, carbon oxidation was minimized when bioflocculation was not limited (0.52-0.95 OUR ratio) and increased otherwise.
- A fully automated control concept was piloted, also a more simplified semi-automated option was proposed.
- Wasting control strategies with bioflocculation boundaries improved effluent quality while meeting carbon capture goals.
- Bioflocculation boundaries are easily applied to current wasting control schemes applied to HRAS systems (i.e. MLSS, SRT, OUR controls).

1. Introduction

Combined with carbon-efficient nutrient removal systems (short-cut nitrogen removal), high-rate activated sludge systems (HRAS) provide a major pathway towards energy neutrality as they allow for the redirection of 35-60% of wastewater COD towards energy recovery through anaerobic digestion (De Graaff & Roest, 2012; Rahman et al., 2020). The A-stage of the AB-process is a HRAS process with very short SRT (0.3-0.5 days) combined with a high loading rate (>2 kg COD kg VSS^{-1} d^{-1}) that minimizes oxidation and maximizes sorption onto sludge. Carbon redirection denotes the transformation of organic carbon (particulates, colloids, and soluble) from wastewater into the sludge matrix through biosorption (i.e., extracellular adsorption, enmeshment, and intracellular storage) and microbial growth phenomena (Rahman et al., 2016). Subsequently, carbon capture denotes the recovery of particulate carbonaceous organics through settling and wasting of the activated sludge, which then has the potential to be used for energy recovery in the form of biogas production in an anaerobic digester. Thus, good bioflocculation and settling behaviour in HRAS systems are essential for successful energy recovery from wastewater.

Reported carbon capture from HRAS varied between 21-55% of total incoming COD (Dai et al., 2018; Dolejs et al., 2016; H. Guven et al., 2017; Jimenez et al., 2015; Meerburg et al., 2015; Rahman et al., 2020) and effluent suspended solids (ESS) from 10 - 120 mg TSS/L (H. Guven et al., 2017; Jimenez et al., 2015; Ngo et al., 2021a; Rahman et al., 2016, 2019; Rahman et al., 2020), indicating that bioflocculation is variable and a function of sludge retention time (SRT), organic loading rate, wastewater composition, reactor configuration, and environmental conditions (Rahman et al., 2020). Recently, high-rate contact-stabilization (CS) was able to mitigate this issue by imposing a feast-famine regime through recycled activated sludge (RAS) aeration (famine) before contacting the sludge with the wastewater (feast). The latter triggered an extracellular polymeric substances (EPS) response, improving bioflocculation, which led to improved carbon capture, lower ESS, and lower threshold of flocculation (TOF) (Rahman et al., 2017). In addition, a high-rate CS configuration showed lower carbon oxidation and thus energy input to achieve similar carbon capture than conventional HRAS systems when operated under similar organic loading rate and SRT (Rahman et al., 2019). Recently, high-rate CS was implemented in secondary treatment at Blue Plains Advanced Wastewater Treatment Plant providing significant improvement in effluent quality, clarifier performance, and energy efficiency (Ngo et al., 2021b). Wett et al. (2020) have also implemented this approach of contact stabilization process in existing primary clarifiers in the AAA process by operating the contact and stabilization parts in a time-sequenced mode. This approach has led to enhanced bioflocculation relative to a more conventional A-stage process or primary clarifiers. Furthermore, the approach of feeding through a settling blanket in the contact mode also achieved desired physical contact to enhance flocculation and achieved 75% COD capture (Wett et al., 2020).

In addition, bioflocculation has shown to deteriorate at shorter SRT (Dai et al., 2018; Faust et al., 2014; Jimenez et al., 2015; Rahman et al., 2020; Van Dierdonck et al., 2012), and when the food to microbe (F/M) ratio drops below an unknown critical threshold (Rahman et al., 2016; Stum & De Clippeleir, 2020). In contrast, the current practice relies on a standard aerobic SRT target of 0.2 days (De Graaff & Roest, 2012), which does not result in optimized bioflocculation performance or energy balances. The high variability in the effluent quality of HRAS systems is one of the reasons why primary clarifiers are often preferred over HRAS systems despite their lower carbon capture.

Despite many advances in process control for nutrient removal (Le et al., 2018; Palatsi et al., 2021; Regmi et al., 2014, 2015; Zhu et al., 2017), process control for HRAS systems has been basic and not optimized for optimal energy or carbon management. Recent studies mainly focused on SRT control (Lee et al., 2007; Olsson et al., 2015; Seuntjens et al., 2020; Wu et al., 2011; YSI, 2014), but the latter is barely used in practice due to the need for several TSS probes and thus added complexity versus the widely used mixed liquor suspended solids (MLSS) control. Miller et al. (2017) explored the possibility of using MLSS-based wasting control to minimize variability in the COD removal efficiencies and bioflocculation. The study concluded that maintaining an MLSS concentration setpoint rather than having an SRT target delivered a more effective approach in maximizing COD removal efficiencies (up to 90%) at DO concentrations of 0.5-1.3 mg O_2/L (Miller et al. 2017). However, the study showed high variability in effluent quality, especially in colloidal COD, and thus indicated that such controls do not optimize for bioflocculation.

As an alternative, the use of oxygen uptake rate (OUR) as a control variable for management of sludge wasting rather than SRT or MLSS targets was shown to result in more direct control of energy input and thus COD oxidation management, which further increased the energy efficiency of plants (Van Winckel, 2019; Van Winckel et al., in review). Moreover, when the OUR setpoint was chosen correctly, bioflocculation was better managed, resulting in stable COD redirection and capture. However, given that the loading rate and environmental conditions dictated the biomass inventory and degree of bioflocculation, these parameters fluctuated dramatically even at stable OUR (Van Winckel, 2019; Van Winckel et al., in review).

Previous studies showed bioflocculation is a dynamic process (Ngo et al., 2021a; Rahman et al., 2016). Thus, one specific SRT, MLSS, or OUR setpoint for wasting control cannot be applied widely over different wastewater treatment plants to achieve similar and stable effluent quality. In addition, daily, weekly, or seasonal changes in wastewater characteristics and operational conditions (MLSS, oxygen levels, temperature, surface overflow rates, solids loading rates) will significantly impact the floc formation and the capture within the clarifiers. Thus, optimal wasting targets or setpoint for these different wasting control strategies will have to be adjusted noticeably in the function of the conditions driving bioflocculation. So far, no online control concept exists that directly controls and manages bioflocculation, and this was therefore the focus of this study.

The study aimed to develop an online bioflocculation control by determining online detection of bioflocculation limitations to manage wasting target. The proposed control concept prioritizes meeting effluent TSS targets before enhancing carbon redirection and energy balances. The hope is that such a control approach can better stabilize effluent quality from HRAS systems and enhance process reliability. This study included the following aspects: (i) the bioflocculation limitation indicators were developed based on 600 days of HRAS pilot runs under different OUR with various bioflocculation conditions; (ii) the process control concept was laid out; (iii) proof of principle of the proposed concept was performed on the OUR-based wasting control and simplified waste flow rate control to show global applicability and impact on effluent total suspended solids (ESS), clarifier capture efficiency, and carbon capture achieved. This study shows for the first time an online control approach directly tailored to managing the settling behaviour of activated sludge.

2. Materials & Methods

2.1 Pilot system

A high-rate activated sludge pilot (V = 1402 liters) was operated at Blue Plains Advanced Wastewater Treatment Plant in Washington (AWWTP), DC, USA. The pilot was operated in a contact-stabilization (CS) configuration and continuously fed with fresh chemically-enhanced primary treatment (CEPT) effluent originating from the full-scale plant at Blue Plains. The CEPT effluent was pumped continuously to the pilot to keep composition as close as possible to the full-scale facility and avoid storage. Details of wastewater influent characteristics are described in table 1. The system was inoculated with high-rate secondary sludge from the Blue Plains AWWTP, which operated under an average SRT of 1.5±0.8 days aimed to maximize carbon capture to anaerobic digestor for methane gas. The CEPT effluent was fed into the contactor (V = 223 liters) reactor for a total HRT of 36 minutes and targeted DO at 0.5 mg O_2/L. From the contactor, the sludge was sent into the three clarifiers (Ø = 30.5 cm and V = 302 liters each). The underflows were combined in a return activated sludge (RAS) tank (V = 50 liters) for 20 minutes and subsequently pumped into the stabilizer column (V = 223 L) with the RAS recycle ratio at 60%. Here, the sludge was provided ample DO (> 2 mg O_2/L) and HRT of 96 minutes to oxidize all remaining absorbed organics. Sludge wasting was conducted from the contactor MLSS. Details on configuration and setup are described in Rahman et al., (2016), Van Winckel, (2019), and Van Winckel et al., (in review).

2.2 Online OUR measurement

The online oxygen uptake rates (OUR) of the contactor and stabilizer reactors were automatically calculated via small online ex-situ setups consisting of aeration (1.5 liters) and measurement vessels (300 ml). Every 20 minutes, the sludge from the contactor and stabilizer reactors was pumped for 400 seconds into the setup, filling up both vessels. At the 300 second mark, the vessels were aerated for 100 seconds to increase DO to a minimum of 5 mg O_2/L. It should note that sludge in both vessels were mixing continued and isolated with the ambient air (Figure S4). Afterwards, both air and feed pumps were turned off, and a declining DO curve was generated. The DO data points were captured for 750 seconds via a membrane probe (Atlas Scientific, USA) and were converted to digital signals using the Atlas Scientific EZO™ DO chip, which communicated with an Arduino Mega through a UART protocol. The signals were then sent to MATLAB R2019b, where the corresponding OUR from the logged declining DO slope was calculated. Data quality was checked by calculating the slope for multiple ranges of DO i.e. 5 to 4 mg O_2/L, 4 to 3 mg O_2/L, 3 to 2 mg O_2/L, 4 to 2 mg O_2/L, and so forth (1 – 0 mg O_2/L was not considered due to rate limiting conditions). The slope with the highest R^2 was selected. If the R^2 of all slopes was similar, the 4 – 2 mg O_2/L slope was chosen. If all slopes had a R^2 lower than 0.8, the value of the previous measurement cycle was fed to the controller. More information could be found at Van Winckel, (2019), Van Winckel et al., (in review) and supplemental Figure S4.

2.3 Controller

The pilot system was operated under OUR-based wasting control (scenario A), OUR-based wasting control with bioflocculation boundaries (Scenario B), and wasting flow control with bioflocculation boundaries (Scenario C). Scenario A was used to identify bioflocculation limitation boundaries and acted as the baseline scenario. Detailed control logic overviews are provided in Figure 3.

2.3.1 Baseline testing without bioflocculation boundaries (Scenario A)

During this scenario, the wasting pump was controlled to meet a given OUR setpoint for the contactor (Figure 3A). The calculated OUR value (measured variable) was subjected to a one-hour rolling average, then compared to the control setpoint and fed to the proportional/integrative (PI) controller in

Matlab Simulink. The PI controller calculated the number of seconds the sludge waste pump had to run per hour in order to achieve a target averaged waste flow rate (control variable). This control approach was first tested by Van Winckel et al. (2019) and Van Winckel et al. (in review), where more details can be found. When the OUR setpoint was lower than the contactor OUR, the waste flow rate increased. Details of the test conditions are addressed in table 1 and table 2.

The measured OUR of the contactor reactor was first subjected to a one-hour rolling average before sending to the PID controller to allow for smoothening out of the signal. P, I, and D values used during the scenario were 750, 0.025, and 0, respectively, resulting in low errors between OUR measured and OUR target. During this scenario, OUR setpoints were changed on a regular basis to push the system and understand when bioflocculation limitations occurred.

2.3.2 Dynamic wasting control with bioflocculation boundaries (scenario B and C)

The control system adjusted OUR setpoints or waste flow setting based on bioflocculation behavior as depicted in Figure 3B and Figure 3C. When the OUR ratio between contactor versus stabilizer was within the upper and lower limit, no bioflocculation limitation was detected, and OUR setpoints were decreased (Figure 3B), or waste flow setpoints were increased (Figure 3C). Outside this OUR ratio range, an opposite trend in OUR or waste flow rates were applied to allow more carbon oxidation and enhance bioflocculation first (Figure 3B and 3C).

The degree of OUR setpoint change depended on how far one operated from the bioflocculation boundaries, and a linear gain factor was applied to control rate of change in case of the OUR control example (Figure 3B). As sludge wasting was a quicker process than microbial growth, a quicker response for decreasing wasting (increased gain factor A versus B) was deemed appropriate to minimize the chance of a complete sludge washout when bioflocculation was limited. The gain factors A and B were 2 and 0.5, respectively for scenario B1. Both A and B were set to 1 during scenario B2. Scenario B1 and B2 followed the same control logic but represented different wastewater characteristics (Table 1). For scenario C, a simplified concept was tested where a step change in waste flow rate setting of 80 L/d was proposed that represented a potential change in SRT of approximately 0.1 days. This change was only made on a daily basis and based on a triplicate OUR ratio measurement during the day rather than online OUR ratio data collection. Scenario C was tested to see if the concept could be scaled down to a semi-online concept if online implementation of OUR ratios was deemed too complicated in practice.

For Scenario B, OUR setpoints were adjusted every 20 minutes as new OUR data was provided. The OUR ratio signal was smoothed out by taking an one hour rolling average of the contactor data to avoid instabilities in control response. It should be noted that P and I parameters were set at 75 and 0.025, respectively, based on two weeks of tuning before the start of the B scenario (data not shown). The fast response of the system to control targets was confirmed under the given tuning conditions.

2.4 Experimental methods

Twenty-four-hour composite samples were collected for the influent and effluent, and grab samples were collected from the contactor and stabilizer on a daily basis. Influent, effluent and contactor samples were analyzed for total (tCOD), particulate (pCOD), colloidal (cCOD), and filter-flocculated COD (ffCOD) fractions. The ffCOD was assessed by following Mamais et al. (1993) method (ZnSO4 flocculated and 0.45 μm filtered). The ffCOD was considered a true soluble COD, and the difference between ffCOD and 1.5 μm glass microfiber filtered COD indicated the colloidal COD (cCOD) fraction. In contrast, the difference between tCOD and 1.5 μm glass microfiber filtered COD indicated the particulate COD (pCOD) fraction. COD, total phosphorus (TP), ortho-phosphorus (OP), and Ammonia (NH_3-N) levels were tested via HACH test kits and HACH DR 2800 spectrophotometer (HACH, Loveland, CO, USA). In addition to the mentioned samples, grab samples for RAS, stabilizer, and ESS from three clarifiers were also collected to assess the total suspended solids (TSS) measured by standard methods (APHA, 2005).

2.5 Mass balance calculations

For COD mass balance, particulate COD leaving the system was categorized as biomass instead of the particulate substrate (Meerburg et al., 2015, Rahman et al., 2016), and carbon redirection was assessed from the carbon mass balance over the reactor from the gathered daily performance data. The formula used for COD fractionations was similar to the calculations used in the studies of Rahman et al. (2016) and Van Winckel et al. (2019). Detail of the calculations are described in the equation 1 to 5 in supplemental information S5.

2.6 Statistical analysis

The statistical differences among the three bioflocculation parameters and different pilot runs were calculated using an unpaired t-test. T-tests with a p-value < 0.05 were identified as statistically significant.

3. Results & Discussion

3.1 Defining bioflocculation targets for HRAS systems (scenario A)

The main objective of the initial operation was to push the system towards increased carbon redirection, decreased OUR, and decreased SRT. By doing so, bioflocculation was challenged as previously observed (Jimenez et al., 2015; Rahman et al., 2016), resulting in a decreasing trend of carbon capture and TSS capture in the clarifier and an increasing trend in effluent suspended solids (ESS) concentration. Failure of bioflocculation was characterized by the inability to waste and thus a complete loss of COD capture even though organic loading rates were maintained and wasting control was activated. Given the diverse environmental and loading conditions during the 600 days (534 data points) high-rate CS pilot run (Table 1) and the constant push of the system towards failure by setting changes in OUR targets, a broad range of conditions that led to bioflocculation limitation were captured in the dataset and shown in Table 1. This led to an average 12 ± 15% COD capture, 58 ± 24 mg TSS/L ESS and 73 ± 22% TSS capture over the clarifier (Table 2 and Figure 1). It must be noted that the fundamental interest of the iterative approach was not to achieve a good and consistent bioflocculation but rather to understand and determine the critical conditions that induce bioflocculation limitation. By acknowledging these conditions, early indicators can be identified and thus may be used to develop online bioflocculation control approaches.

The obtained data was further used to identify the definition for this system of good and limited bioflocculation conditions. To do so carbon capture, which is directly dependent on the bioflocculation behavior and entails the main function of the high-rate system (Rahman et al., 2020), was used as the main criteria to differentiate the bioflocculation conditions. Only at a carbon capture target of 31%, a significant impact on ESS ($p < 0.05$) and TSS capture over the clarifier ($p < 0.1$) was observed (Figure 1, Table 2). At carbon capture above 31%, average of ESS levels were lower at 38±18 mg TSS/L instead of 61±23 mg TSS/L, and average of TSS capture over the clarifier was 84±11 instead of 79±16% (Figure 1). Boxplot in Figure 1 also showed a clear differentiation between in ESS and TSS capture in clarifier at the threshold of COD capture at 31%. In addition, the good bioflocculation dataset was characterized by significantly ($p<0.05$) shorter SRT, lower carbon oxidation, MLSS, effluent total, and particulate COD (Table 1 and 2). Conventional feast-famine parameters defined on either soluble or total COD over biomass present were not sensitive enough to be directly linked to bioflocculation conditions ($p < 0.05$, Table 1) despite literature emphasizing the importance of feast-famine for improved settleability (Sturm & De Clippeleir, 2020). It should be noted that the probability of achieving bad bioflocculation was high in the overall data set, and good bioflocculation only represented 15% of the used data set (Table 1).

Overall, the following differentiating criteria were defined to achieve good bioflocculation: (i) COD capture above 31%, (ii) effluent suspended solids (ESS) below 48 mg TSS/L as defined by the overlap of the 75^{th} percentile of the good and the 25^{th} percentile of the bad bioflocculation data, and (iii) a TSS capture over the clarifier above 78%, as defined by the 25^{th} percentile of good bioflocculation dataset (Figure 1). It should be noted that the COD capture criteria for the pilot system was lower compared to data from full-scale HRAS systems treating raw sewage with typical carbon capture around 25-74% COD capture. The latter is a result of the difference in wastewater characterization (Rahman et al., 2020). For the effluent solids and clarifier capture criteria, targets defined based on the pilot system fall within full-scale results reported by De Graaff & Roest (2012) and are thus more globally applicable.

3.2 Development of bioflocculation boundaries for limitation detection

It was hypothesized that bioflocculation would remain efficient even under low SRT when a sufficient feast-famine regime is applied. Increased feast-famine was shown to induce EPS production in high-rate CS systems (Meerburg et al., 2016; Rahman et al., 2017) and A stage systems (Jimenez et al., 2015; Rahman et al., 2019). In addition, the EPS response as a function of the feast-famine regime was directly linked to the formation of denser sludge and granule formation (Sturm & De Clippeleir, 2020). Feast-famine was defined in the latter study by the added readily biodegradable COD (rbCOD) compared to the present biomass concentration (in VSS). As online rbCOD measurements are not available, online control to a specific feast-famine level is not practically feasible. In addition, data based on scenario A did not clearly show a link between traditional feast famine parameters and bioflocculation behavior (Table 1). This indicated that measuring a direct microbial response might entail better information. This study proposed the use of the ratio between contactor and stabilizer OUR as an online but analog signal for the activity in the contactor (feast) versus stabilizer (famine). This OUR ratio represented the microbial response more directly and was hypothesized to represent the feast famine condition of the system and would therefore play a direct role in bioflocculation (Sturm and De Clippeleir, 2020). Rahman et al. (2017) showed the link between this OUR ratio and the EPS response from stabilizer to contactor and its impact on the amount of carbon captured. This work aimed to translate this observation into a viable online control system tailored to optimizing bioflocculation. The overall control concept of inclusion of bioflocculation boundaries on top of wasting control strategies is shown in Figure 3. The upper and lower bioflocculation boundaries were defined based on baseline data available during scenario A.

3.2.1 Upper bioflocculation limit

A high OUR ratio would indicate a high feast-famine regime and thus beneficial conditions for bioflocculation. However, the OUR ratio can also increase substantially when the active biomass fraction or MLSS drops to lower numbers. Biomass limitation can lead to decreased COD removal and/or EPS production as well as decreased bioflocculation due to the limited number of collisions. The pilot often experienced MLSS limitation due to low-strength wastewater fed to the pilot and limited the organic loading due to hydraulic limitation as a result of limited clarifier surface. This resulted in a median MLSS concentration during scenario A of 350 mg TSS/L. Table 1 also shows slightly increased OUR ratios in the limited bioflocculation group compared to the good bioflocculation group, indicating that an upper OUR ratio boundary might be needed to avoid such flocculation limitations (Table 1).

The probability of achieving good bioflocculation (COD capture > 31%, ESS < 48 mg TSS/L, and TSS capture in clarifier > 78%) , as defined in section 3.1, given a maximum OUR ratio target, is presented in Figure 2A. The chance of achieving the desired bioflocculation decreased at OUR ratios above 0.95. The latter OUR ratio target coincided with a decrease in median MLSS levels (Figure 2B) and thus confirmed potential biomass limitation. All analyses considered, the upper bioflocculation was set at 0.95, and this target was implemented within the control scheme (Figure 3).

3.2.2 Lower bioflocculation limit

Wet weather events decreased the OUR ratio by diluting the readily biodegradable COD in the influent and decreasing the biomass activity in contactor. The pilot system emphasized the latter events as it operated under constant hydraulic load rather than increased hydraulic load during full-scale wet weather events. Without a lower bioflocculation boundary, the controller would push down the OUR setpoint and thus increase wasting in an attempt to increase feast famine regime, and by doing so risk biomass washout due to a lack of substrate availability (feast potential) in the wastewater. The wet weather modus operandi in full-scale plants entails protecting biomass inventory by bypassing certain reactor zones and/or decreasing airflow rates during aeration (EPA, 2014). In this pilot influent flow rates were kept constant, and thus surface overflow rates on the clarifiers did not change, neither did the operational strategy change during those events. Based on the dataset of various rain events 132 data points of the OUR ratios at dry and wet weather events were separated described in Figure 2C. Wet weather event periods were detected by plant influent flows to the full-scale WRRF below and above 1400602 m^3/d (370 MGD), respectively. An OUR ratio of 0.52 separated out the OUR ratios obtained between dry and wet weather events, and such low OUR ratios were thus resulting from diluted wastewater loading (75^{th} of during wet weather event, $p < 0.05$ with before wet weather event (Figure 2C)). An OUR ratio of 0.52 was chosen as the lower OUR boundary, and this target was implemented within the control scheme shown in Figure 3.

3.3 OUR control with bioflocculation boundaries (Scenario B): full automated example

This scenario was a fully automated scenario in which all parameters were collected, and all process control decisions were made automatically every 20 minutes (Figure 3). It was envisioned that although tested here on an OUR-based wasting strategy, the same concept could be applied for MLSS-based wasting (Miller et al., 2017) or SRT-based wasting (Olsson et al., 2015; YSI, 2014) using online TSS probes. Scenario B was split up into two scenarios based on wastewater characterization. The organic loading rate during scenario B1 was statistically lower than reference scenario A due to diluted wastewater characteristics (Table 1, Figure 4D, and 5B). The decreased total COD loading rate might have impacted the bioflocculation behavior during scenario B1, and the lower overall solids loading might have favored decreased effluent suspended solids (Rahman et al., 2016; Van Winckel et al., 2018). Scenario B2, although representing a shorter period, had similar wastewater characteristics than the reference scenario A and overcame this potential impact (Table 1).

Figure 4 shows the detailed trends in OUR ratios during scenario B1 leading to detection of bioflocculation limitations, and as a result, the control responses in terms of OUR setpoint and wasting flow rate. From day 652 to 656 and 667 to 670 OUR ratios were mostly above the upper bioflocculation boundary (OUR ratio > 0.95), thus control eventually increased the OUR setpoint up to the maximum (Figure 4A and 4B). This action allowed the system to slow down wasting (Figure 4C) and thus allowed for increased carbon oxidation from 11 % on day 667 to 53% on day 669 (Figure 4E). The latter maintained good effluent quality (< 30 mg TSS/L) and TSS capture (> 90%) despite bioflocculation limitation (Figure 4G and 4H). Rahman et al. (2020) pointed that optimal carbon oxidation is needed for achieving good effluent quality, and TSS capture as a certain amount of oxidation may be required to provide a sufficient level of EPS production and as a consequence floc structure (Jimenez et al., 2015; Rahman et al., 2016). Effluent would have deteriorated without the increased carbon oxidation as observed during reference scenario A. On the other hand from day 671 to 686, OUR ratios were frequently at optimal range (OUR ratio within 0.52-0.95), so the controller decreased OUR setpoint to target a lower optimal range of carbon oxidation (Figure 4A), resulting in more carbon capture and capture efficiency (Figure 4E and 4F), while ESS and TSS capture were maintained in a good range (Figure 4G and 4H). Overall, this approach was able to meet the target good bioflocculaiton criteria with low ESS of 17±6.9 (mg TSS/L), improved TSS capture of 95±3.9(%), and COD capture of 31±15 (%) (Table 2). This was on all three fronts a significant improvement compared to the same control OUR wasting control approach without the bioflocculation boundaries (Table 2).

Given the lower organic loading during scenario B1, system output was collected for a second period (scenario B2) with higher organic loading similar to the baseline scenario A, with the exception of an increased pCOD/tCOD during scenario B2 ($p < 0.05$). Operational details are shown in Figure S1 and Table 1. Overall, all bioflocculation criteria were also met during this run (Table 2). While both the good bioflocculation data set for scenario A and scenario B2 observed the similar carbon redirection level, the high fraction of pCOD/tCOD in the influent potentially caused poorer effluent quality and COD capture in scenario B2 (Table 2, Figure 7). Increased particulate COD loading to HRAS systems was previously described to accelerate saturation of sorption spots (Van Winckel et al., 2018) and thus might impact bioflocculation and bioflocculation limitation significantly. Even though pCOD was driving some of the ESS levels, even under more challenging conditions in scenario B1, significantly lower ESS and better TSS capture were obtained under the newly proposed control scheme versus the OUR-based wasting control without bioflocculation boundaries (Scenario A) (Table 1, Figure 7). This result confirmed the need for dynamic wasting targets in the function of bioflocculation conditions to achieve more controlled outputs in terms of effluent quality. The achieved better bioflocculation could potentially reduce energy demand through better sorption of colloids and surfactants (Garrido-Baserba et al., 2020), which can further enhance the energy mass balance of the high-rate CS system. In addition, good and stable effluent quality also created increased stability for downstream nutrient removal processes as more stable effluent COD/N ratios were established.

3.4 Wasting flow control with bioflocculation boundaries (scenario C): simplified control example

Even though PID control has long been developed and has been accepted as standard practice, an IWA report showed that about 50% of the WRRF run their systems in manual mode rather than turning on the PID control loops due to the complexity of tuning, poor sensor choice, high maintenance, and/or the human aspect of the control systems (Olsson et al., 2015). Therefore, a simplified version of the online bioflocculation control was tested to see what benefits could be obtained when a simplified control approach was applied (Figure 3C).

The pilot system was operated for 16 SRT cycles under this control scheme (Figure 5). Influent characterization (concentration or COD fractions of PE) was similar between scenario C, scenario B2, and the baseline scenario A, as well as the good bioflocculation dataset within scenario A ($p>0.05$, Table 1, Figure 5C). During scenario C, optimal bioflocculation conditions (OUR ratio within 0.52-0.95) were observed for the first six days (Figure 6A); hence the control increased wasting flow rate, allowing more carbon capture, capture efficiency and lower carbon oxidation (Figure 5C and 5D). However, the system was pushed more and more towards bioflocculation limitation from day of 734 to 739 (OUR ratio > 0.95, Figure 5A) as a result of increased wasting and a sudden increase in particulate COD loading (Figure 5B), again indicating the sensitivity of bioflocculation for oversaturation of sorption spots (Van Winckel et al., 2018) and limitation in EPS (Jimenez et al., 2015; Rahman et al., 2016). As the OUR ratio reached the maximum boundary, the control slowed down the wasting flow rate permitting more carbon oxidation to enhance bioflocculation, and bioflocculation was restored at the end of the experiment (Figure 5A, 5B, 5C, and 5D). It should be noted that the system took seven days to reach optimal bioflocculation levels again (Figure 5A) as a result of the slow decision-making (every 24 hours) and offline OUR measurement (3 grab samples). An increased step-change might have accelerated the recovery; however, this might have decreased control stability (Nise et al., 2011; Olsson et al., 2015). Alternatively, the frequency of grab sampling and decision-making could have been accelerated. However, this would put a larger workload on the operator and make this approach impractical when no online OUR sensor is installed. It should be noted that OUR measurements taken for flocculation boundary measurements were based on an ex-situ declining DO experiment and one can explore the use of calculated OUR from field airflow and DO data as an alternative.

Despite the simplification and slow control adjustments compared to scenario B, improved consistency and quality in ESS, TSS capture, and COD capture were achieved (Figure 5, 6 and Table 2). In addition, scenario C scored better in all three bioflocculation criteria than the baseline scenario A (Figure 6). This showed that the concept was strong enough to work under simplified and slower control action.

3.5 Impact of bioflocculation boundaries on control of high-rate CS systems

Data from full-scale and pilot-scale systems showed high variability in bioflocculation outcomes with ESS and COD capture fluctuating in a range of 10 – 120 mg TSS/L (H. Guven et al., 2017; Jimenez et al., 2015; Ngo et al., 2021a; Rahman et al., 2016, 2019; Rahman et al., 2020) and 21-55% (Dai et al., 2018; Dolejs et al., 2016; H. Guven et al., 2017; Jimenez et al., 2015; Meerburg et al., 2015; Rahman et al., 2020), respectively. This lined up with the significant variation of ESS (7 to 113 mg TSS/L), TSS capture in clarifier (51 to 98%), and COD capture (median at 12% and varied from 0 to 49%) in scenario A with no bioflocculation control (Figure 6). The proposed control approach with bioflocculation boundaries showed both in fully automated (scenario B) as well as a simplified version (scenario C) improved ESS levels (< 50 mg TSS/L) and reliability of ESS numbers (Figure 6). Similarly, TSS (> 90%) and COD capture (median at 32%) were improved and stabilized as well (Figure 6). The increased carbon oxidation applied when bioflocculation limitation was detected (outside bioflocculation boundaries) did not increase overall carbon oxidation levels on average basis, but rather increased overall carbon capture levels as bioflocculation limitation were resolved quickly. Depending on the variability of the bioflocculation efficiency, the range of carbon capture was wider or smaller; however, this study showed that a minimum level of carbon recovery could be maintained at all times based on the proposed control approach in contrast to control systems without bioflocculation boundaries (Figure 6). Table 2 also illustrated that higher total COD removal was observed when control applied bioflocculation boundaries to compare with baseline scenario. Overall, effluent tCOD of scenario B1 (81 ± 14 mg/L), B2 (127 ± 31 mg/L), and C (118 ± 31 mg/L) with bioflocculation control captured lower range and more stable to compare with scenario A (170 ± 53 mg/L) (Table 2). The latter helps WRRF achieve the needed energy recovery (Sancho et al., 2019). In addition, it should be noted that the lower and more reliable ESS has an additional energy benefit as biodegradable COD is slowly added to the downstream biological nutrient removal system where oxygen might be used to oxidize (part of) it (Sancho et al., 2019).

From a control standpoint, scenario B and C showed increased process stability compared to scenario A, especially in terms of clarifier performance. Increased process efficiency and stability generated in this study shows similarities with nutrient removal control systems. For example, when AvN control, a control principle focused on process efficiency, is used by itself, it showed efficient total nitrogen removal, but effluent quality could not be guaranteed (Regmi et al., 2015). In contrast, ammonium-based aeration control (ABAC) guarantees effluent quality but not necessarily process efficiency (Rieger et al., 2014). When ammonium boundaries were added to AvN control, nitrogen removal was optimized as long as ammonium limits were met and both efficiency and effluent goals were optimized (communication with Bernhard Wett). The proposed approach of adding bioflocculation boundaries to wasting strategies provided similar benefits of achieving effluent quality while reaching the best COD mass balance. In addition, the latter hybrid control systems showed increased control stability compared to the OUR control only (Van Winckel, 2019; Van Winckel et al, in review) or AvN control only (communication with Bernhard Wett).

It should be noted that the transferability of the exact boundary levels (0.52-0.95) as used in this study will need to be evaluated when applied to a new condition or systems. In addition, depending on the response time of the system as well as system dynamics, the gain factors will need tuning in new systems.

One challenge of the proposed approach was the high maintenance needs for OUR measurements. We chose to measure OUR based on an external measurement loop to allow for a standardized OUR measurement independent of diffusers or oxygen transfer changes inside the system (Van Winckel, 2019; Van Winckel et al, in review). In addition, to allow for fast response, a membrane probe was used rather than an LDO probe, which required more frequent cleaning due to the sensitivity of the membrane to fouling (Hach LDO manual, 2006; Atlas scientific membrane EZO manual, 2017). Due to the smaller setup, no automatic cleaning (mechanical or air sparge) was feasible. Probes were maintained on every 12 to 24 hour to maintain reliable data collection. Future work will need to look at online OUR measurement probes with improved self-cleaning and calibration (APS-TOX manual, 2019) or alternative ways of measuring the bioflocculation boundaries or OUR. This could include calculation of OUR in-situ, based on applied airflow rates, or by applying intermittent aeration. The latter approaches were applied in other studies to improve nitrogen removal (Baeza et al., 2002; Jubany et al., 2009; Surmacz-Gorska et al., 1996), but never tested for HRAS where faster OUR rates and more dynamics in oxygen transfer rates might exist (Garrido-Baserba et al., 2020). Alternatively, other factors that can detect the feast famine level and microbial response similar to OUR might result in the same level of bioflocculation limitation detection. Overall, identifying a reliable bioflocculation boundary detection method is crucial step to bring this concept to practical application.

4. Conclusion

This study proposed a control strategy using bioflocculation boundaries for wasting control strategy to enhance effluent quality and effluent stability while still meeting carbon capture goals. The bioflocculation boundaries were based on feast famine detection in the high-rate contact stabilization through measurements of the OUR ratio between contactor and stabilizer. Carbon oxidation was minimized within bioflocculation boundaries of 0.52-0.95 OUR ratio and increased outside these boundaries to maintain effluent quality. Both an online dynamic OUR-based wasting control with bioflocculation boundaries (a fully automated application) as well as a wasting flow control with bioflocculation boundaries (a simplified application) were evaluated. A significant improvements in ESS stability and level

(< 50 mg TSS/L), TSS capture (>90%), and COD capture (median at 32%) were achieved with this new control approach. It should note that bioflocculation boundaries can be easily applied to current wasting control schemes applied to HRAS systems (i.e. MLSS, SRT, OUR controls) and thus might have broad applicability. The translation of this concept to a practical application will depend on finding a reliable bioflocculation boundary detection method and this will need to be the focus of future work. This study shows how one can overcome the process stability challenges of current HRAS systems and provide a path to achieve more reliable outcomes.

5. Acknowledgements

This work was supported by District of Columbia Water and Sewer Authority (DC Water), Washington, DC, USA. The authors gratefully thank Norman Dockett for technical support and everyone in the DC Water research lab for all assistance offered.

6. References

APHA. (2005). Standard Methods for the Examination of Water and Wastewater, 21st ed. APHA:Washington, DC, USA, 2005. *American Water Works Association/American Public Works Association/Water Environment Federation*, *51*(6).

Baeza, J. A., Gabriel, D., & Lafuente, J. (2002). In-line fast OUR (oxygen uptake rate) measurements for monitoring and control of WWTP. *Water Science and Technology*, *45*(4–5), 19–28.

Dai, W., Xu, X., & Yang, F. (2018). High-rate contact stabilization process-coupled membrane bioreactor for maximal recovery of organics from municipal wastewater. *Water (Switzerland)*, *10*(7).

De Graaff, M. and Roest, K. (2012). Inventarisatie van AB-systemen - optimale procescondities in de A-trap. KWR2012.094.

Dolejs, P., Gotvald, R., Velazquez, A. M. L., Hejnic, J., Jenicek, P., & Bartacek, J. (2016). Contact Stabilization with Enhanced Accumulation Process for Energy Recovery from Sewage. *Environmental Engineering Science*, *33*(11), 873–881.

EPA. (2014). Summary of Blending Practices and the Discharge of Pollutants for Different Blending Scenarios. No. EP-C-11-009.

Faust, L., Temmink, H., Zwijnenburg, A., Kemperman, A. J. B., & Rijnaarts, H. H. M. (2014). High loaded MBRs for organic matter recovery from sewage: Effect of solids retention time on bioflocculation and on the role of extracellular polymers. *Water Research*, *56*, 258–266.

Garrido-Baserba, M., Rosso, D., Odize, V., Rahman, A., Van Winckel, T., Novak, J. T., Al-Omari, A., Murthy, S., Stenstrom, M. K., & De Clippeleir, H. (2020). Increasing oxygen transfer efficiency through sorption enhancing strategies. *Water Research*, *183*, 116086.

Guven, H., Ersahin, M. E., Dereli, R. K., Ozgun, H., Sancar, D., & Ozturk, I. (2017). Effect of Hydraulic Retention Time on the Performance of High-Rate Activated Sludge System: a Pilot-Scale Study.

Water, Air, and Soil Pollution, *228*(11).

Jimenez, J., Miller, M., Bott, C., Murthy, S., Clippeleir, H. De, & Wett, B. (2015). *High-rate activated sludge system for carbon management e Evaluation of crucial process mechanisms and design parameters*. 1–7.

Jubany, I., Lafuente, J., Baeza, J. A., & Carrera, J. (2009). Total and stable washout of nitrite-oxidizing bacteria from a nitrifying continuous activated sludge system using automatic control based on Oxygen Uptake Rate measurements. *Water Research*, *43*(11).

Le, T., Fofana, R., Massoudieh, A., Al-Omari, A., Murthy, S., Wett, B., Chandran, K., DeBarbadillo, C., Bott, C., & Clippeleir, H. De. (2018). Achieving low TN effluent by operating AvN control coupled with partial denitrification-anammox control. *Proceedings of the Water Environment Federation*, *2018*(5).

Lee, D., Kim, M., & Chung, J. (2007). Relationship between solid retention time and phosphorus removal in the anaerobic-intermittent aeration process. *Journal of Bioscience and Bioengineering*, *103*(4).

Mancell-Egala, W. A. S. K., De Clippeleir, H., Su, C., Takacs, I., Novak, J. T., & Murthy, S. N. (2017). Novel Stokesian Metrics that Quantify Collision Efficiency, Floc Strength, and Discrete Settling Behavior. *Water Environment Research*, *89*(7), 586–597.

Hatch LDO manual, (2006). LDO ™ Dissolved Oxygen Sensor manual.

Meerburg, F. A., Boon, N., Van Winckel, T., Pauwels, K. T. G., & Vlaeminck, S. E. (2016). Live fast, die young: Optimizing retention times in high-rate contact stabilization for maximal recovery of organics from wastewater. *Environmental Science and Technology*, *50*(17), 9781–9790.

Meerburg, F. A., Boon, N., Van Winckel, T., Vercamer, J. A. R., Nopens, I., & Vlaeminck, S. E. (2015). Toward energy-neutral wastewater treatment: a high-rate contact stabilization process to maximally recover sewage organics. *Bioresource Technology*, *179*, 373–381.

Miller, M. W., Elliott, M., DeArmond, J., Kinyua, M., Wett, B., Murthy, S., & Bott, C. B. (2017). Controlling the COD removal of an A-stage pilot study with instrumentation and automatic process control. *Water Science and Technology*, *75*(11), 2669–2679.

Ngo, K. N., Van Winckel, T., Massoudieh, A., Takács, I., Wett, B., Bott, C., Al-Omari, A., Murthy, S., & De Clippeleir, H. (2019). Extracellular polymeric substance composition as a bridge between process and clarifier models. In Proc. WEFTEC 2019, Chicago, USA.

Ngo, K. N., Van Winckel, T., Massoudieh, A., Wett, B., Al-Omari, A., Murthy, S., Takács, I., & De Clippeleir, H. (2021a). Towards more predictive clarification models via experimental determination of flocculent settling coefficient value. *Water Research*, *190*.

Ngo, K.N, Sabur.M, Massoudieh. A, Wett. B, Bott. C, Passarelli. N, Tesfaye. A, Suzuki. R, deBarbadillo. C and De Clippeleir, H (2021b). Improving clarifier performance and capacity through full-scale implementation of high-rate contact stabilization. In Proc. WEFTEC 2021, Chicago, USA.

Nise, N., Perez, M., Perez, A., Perez, E., Nise, N., Simrock, S., Siddique, N., & Carrillo, A. (2011). Control Systems Engineering 6th Edition. In *California State Polytechnic University* (Vol. 6th).

Olsson, G., Nielsen, M., Yuan, Z., Lynggaard-Jensen, A., & Steyer, J.-P. (2015). Instrumentation, Control and Automation in Wastewater Systems. In *Water Intelligence Online* (Vol. 4, Issue 0).

Atlas Scientific EZO Manual, 2017. Atlas scientific dissolved oxygen EZO manual.

Palatsi, J., Ripoll, F., Benzal, A., Pijuan, M., & Romero-Güiza, M. S. (2021). Enhancement of biological nutrient removal process with advanced process control tools in full-scale wastewater treatment plant. *Water Research*, *200*, 117212.

Rahman, A., De Clippeleir, H., Thomas, W., Jimenez, J. A., Wett, B., Al-Omari, A., Murthy, S., Riffat, R., & Bott, C. (2019). A-stage and high-rate contact-stabilization performance comparison for carbon and nutrient redirection from high-strength municipal wastewater. *Chemical Engineering*

Journal, *357*(September 2018), 737–749.

Rahman, A., Hasan, M., Meerburg, F., Jimenez, J. A., Miller, M. W., Bott, C. B., Al-Omari, A., Murthy, S., Shaw, A., De Clippeleir, H., & Riffat, R. (2020). Moving forward with A-stage and high-rate contact-stabilization for energy efficient water resource recovery facility: Mechanisms, factors, practical approach, and guidelines. In *Journal of Water Process Engineering*.

Rahman, A., Meerburg, F. A., Ravadagundhi, S., Wett, B., Jimenez, J., Bott, C., Al-Omari, A., Riffat, R., Murthy, S., & De Clippeleir, H. (2016). Bioflocculation management through high-rate contact-stabilization: A promising technology to recover organic carbon from low-strength wastewater. *Water Research*, *104*, 485–496.

Rahman, A., Mosquera, M., Thomas, W., Jimenez, J. A., Bott, C., Wett, B., Al-Omari, A., Murthy, S., Riffat, R., & De Clippeleir, H. (2017). Impact of aerobic famine and feast condition on extracellular polymeric substance production in high-rate contact stabilization systems. *Chemical Engineering Journal*, *328*, 74–86.

Regmi, P., Holgate, B., Fredericks, D., Miller, M. W., Wett, B., Murthy, S., & Bott, C. B. (2015). Optimization of a mainstream nitritation-denitritation process and anammox polishing. *Water Science and Technology*, *72*(4).

Regmi, P., Miller, M. W., Holgate, B., Bunce, R., Park, H., Chandran, K., Wett, B., Murthy, S., & Bott, C. B. (2014). Control of aeration, aerobic SRT and COD input for mainstream nitritation/denitritation. *Water Research*, *57*.

Rieger, L., Jones, R. M., Dold, P. L., & Bott, C. B. (2014). Ammonia-Based Feedforward and Feedback Aeration Control in Activated Sludge Processes. *Water Environment Research*, *86*(1), 63–73.

Sancho, I., Lopez-Palau, S., Arespacochaga, N., & Cortina, J. L. (2019). New concepts on carbon redirection in wastewater treatment plants: A review. *Science of the Total Environment*, *647*, 1373–

1384.

Seuntjens, D., Carvajal Arroyo, J. M., Van Tendeloo, M., Chatzigiannidou, I., Molina, J., Nop, S., Boon, N., & Vlaeminck, S. E. (2020). Mainstream partial nitritation/anammox with integrated fixed-film activated sludge: Combined aeration and floc retention time control strategies limit nitrate production. *Bioresource Technology*, *314*.

Sturm. B & De Clippeleir. H., (2020). Balancing Flocs and Granules for Activated Sludge Process Intensification in Plug Flow Configurations. Project N_0. U1R14/4870, Water Research Foundation.

Surmacz-Gorska, J., Gernaey, K., Demuynck, C., Vanrolleghem, P., & Verstraete, W. (1996). Nitrification monitoring in activated sludge by oxygen uptake rate (OUR) measurements. *Water Research*, *30*(5), 1228–1236.

Van Dierdonck, J., Van Den Broeck, R., Vervoort, E., D’Haeninck, P., Springael, D., Van Impe, J., & Smets, I. (2012). Does a change in reactor loading rate affect activated sludge bioflocculation? *Process Biochemistry*, *47*(12), 2227–2233.

Van Winckel, T., 2019. *Towards intensification of water resource recovery facilities: smart kinetic and physical selection for design and control of mainstream processes.* Ghent University, Belgium. PhD Thesis.

Van Winckel, T., Olagunju, O., Sturm, B., Jones, K. L., Bott, C., Wett, B., Al-Omari, A., Murthy, S., Vlaeminck, S. E., & De Clippeleir, H. (2022). On-line oxygen uptake rate control leads to stable oxidation and reduced aeration costs in high-rate activated sludge systems. In review.

Van Winckel, T., Liu, X., Vlaeminck, S. E., Takács, I., Al-Omari, A., Sturm, B., Kjellerup, B. V., Murthy, S. N., & De Clippeleir, H. (2018). Overcoming floc formation limitations in high-rate activated sludge systems. *Chemosphere*, *215*, 342–352.

Wett, B., Aichinger, P., Hell, M., Andersen, M., Wellym, L., Fukuzaki, Y., Cao, Y. S., Tao, G., Jimenez, J., Takacs, I., & Bott, C. (2020). *Operational and structural A-stage improvements for high-rate carbon removal*. 1–7.

Wu, C., Peng, Y., Wang, S., Li, X., & Wang, R. (2011). Effect of sludge retention time on nitrite accumulation in real-time control biological nitrogen removal sequencing batch reactor. *Chinese Journal of Chemical Engineering*, *19*(3), 512–517.

YSI. (2014). Implementation of solids retention time (SRT) control in wastewater treatment. *YSI Solid Retention Time White Paper*.

Zhu, Z., Wang, R., & Li, Y. (2017). Evaluation of the control strategy for aeration energy reduction in a nutrient removing wastewater treatment plant based on the coupling of ASM1 to an aeration model. *Biochemical Engineering Journal*, *124*, 44–53.

7. Table and Figure

Table 1: Overview of influent characterization, operational conditions, oxygen uptake rate (OUR) data, and clarifier performance data for the baseline scenario (A) operated with OUR-based wasting control strategy, Scenario B with OUR-based wasting control strategy with added bioflocculation boundaries, and scenario C with a simplified version of control relying on direct waste flow control with bioflocculation boundaries. The details of the control logic are shown in Figure 3. Scenarios with statistically different parameters ($p < 0.05$) share the same letter in superscript.

Characterization	Scenario: A [Baseline: OUR-based wasting control without bi-oflocculation boundaries (BB)]			Scenario: B1 (Dynamic OUR-based wasting con-trol with BB)	Scenario: B2 (Dynamic OUR-based wasting con-trol with BB)	Scenario: C (Wasting flow control with BB)
	All	Limited (85%)	Good (15%)			
Influent Characterization						
tCOD (mg/L)	258 ± 69^{a}	261 ± 71	243 ± 55^{b}	158 ± 22^{ab}	271 ± 52	230 ± 57
pCOD (mg/L)	131 ± 54^{a}	135 ± 54	114 ± 49^{b}	66 ± 17^{ab}	147 ± 32	130 ± 37
cCOD (mg/L)	45 ± 28	44 ± 28	55 ± 28	42 ± 16	50 ± 18	30 ± 21
sCOD (mg/L)	81 ± 21^{a}	82 ± 21	75 ± 23^{b}	50 ± 9^{ab}	75 ± 20	70 ± 20
pCOD/tCOD (%)	51 ± 12^{ab}	51 ± 11^{c}	45 ± 10^{bc}	42 ± 9^{a}	54 ± 7^{b}	57 ± 8
cCOD/tCOD (%)	18 ± 9^{ab}	17 ± 8^{c}	23 ± 11^{b}	36 ± 9^{a}	18 ± 5	12 ± 8^{b}
sCOD/tCOD (%)	32 ± 7	32 ± 7	32 ± 8	32 ± 6	27 ± 5	31 ± 6
TSS (mg TSS/L)	77 ± 51^{a}	79 ± 53	65 ± 32^{b}	38 ± 10^{ab}	73 ± 22	76 ± 22^{ab}
NH_4^+ (mg NH_3-N/L)	30 ± 8^{a}	30 ± 8^{c}	34 ± 8^{bc}	20 ± 7^{ab}	28 ± 8	22 ± 6^{b}
OP (mg PO_4-P/L)	1.2 ± 0.7^{a}	1.2 ± 0.6	1.3 ± 0.5^{b}	0.8 ± 0.2^{ab}	1.7 ± 0.6	1.6 ± 0.6^{ab}
Soluble volumetric loading rate (kg sCOD/m^3/day)	2 ± 0.6^{a}	2 ± 0.7^{c}	1.7 ± 0.6^{bc}	1.2 ± 0.2^{ab}	1.8 ± 0.5^{a}	1.5 ± 0.3^{a}
Total volumetric loading rate (kg tCOD/m^3/day)	6.4 ± 2.3^{a}	6.5 ± 1.9	5.4 ± 1.3^{b}	3.8 ± 0.6^{ab}	6.6 ± 1.3	5.5 ± 1.4^{b}
Operational Conditions						
MLSS (mg TSS/L)	406 ± 276	421 ± 284^{c}	317 ± 207^{bc}	355 ± 85	673 ± 230^{b}	496 ± 119^{b}
SRT_{20} (day)	0.8 ± 0.5^{a}	0.7 ± 0.5^{c}	0.6± 0.4^{bc}	0.8 ± 0.3^{ab}	1.8 ± 0.7^{ab}	0.8 ± 0.3
Temperature (^{0}C)	19 ± 2	19 ± 2	20 ± 1	9 ± 1	10 ± 1	12 ± 1
OUR Data						
OUR ratio (-)	1.3 ± 0.5^{a}	1.2 ± 0.5^{c}	1.1 ± 0.3^{bc}	0.7 ± 0.1^{ab}	0.8 ± 0.2^{ab}	0.9 ± 0.2^{a}
OUR Contactor (mg O_2 L^{-1} h^{-1})	25 ± 15^{a}	25 ± 15	24 ± 10^{b}	10 ± 2.1^{ab}	10 ± 2.1^{ab}	24 ± 10
OUR Stabilizer (mg O_2 L^{-1} h^{-1})	22 ± 13^{a}	22 ± 13	20 ± 11^{b}	15 ± 4^{a}	14 ± 3.5^{a}	29 ± 11^{ab}
Clarifier Operation						
SOR (m/h)	0.8 ± 0.2^{a}	1.1 ± 0.3	0.8 ± 0.3^{b}	1 ± 0.02^{ab}	0.91 ± 0.05	0.93 ± 0.04^{ab}
SLR (kg TSS/m^2/d)	13 ± 3	13 ± 2	12 ± 2.3	8.7 ± 2.1	11 ± 4.4	10 ± 2.1

Table 2: Average levels of bioflocculation criteria, effluent quality, and COD mass balances for the baseline scenario (A) operated with OUR-based wasting control strategy, Scenario B with OUR-based wasting control strategy with added bioflocculation boundaries, and scenario C with a simplified version of control relying on direct waste flow control with bioflocculation boundaries. The details of the control logic are shown in Figure 3. Scenarios with statistically different parameters ($p < 0.05$) share the same letter in superscript.

Characterization	**Scenario**					
	A			**B1**	**B2**	**C**
	Baseline: OUR-based wasting control without bioflocculation boundaries			Dynamic OUR-based wasting control with boundaries)	Dynamic OUR-based wasting control with bounda-ries	Wasting flow con-trol with boundaries
	All	**Limited (85%)**	**Good (15%)**			
Bioflocculation Criteria						
COD capture (%)	12 ± 15[a]	7 ± 9[ac]	41 ± 7[ac]	31 ± 15[a]	35 ± 9[a]	22 ± 10[a]
ESS (mg TSS/L)	58 ± 24[a]	61 ± 23[c]	38 ± 18[abc]	17 ± 7[ab]	43 ± 7[a]	38 ± 8[a]
TSS capture in clarifier (%)	73 ± 22[ab]	79 ± 16[abc]	84 ± 11[abc]	95 ± 4[ab]	93 ± 2.6[ab]	92 ± 2[ab]
Effluent Characterization						
tCOD (mg/L)	170 ± 53[a]	170 ± 54[c]	143 ± 42[bc]	81 ± 14[ab]	127 ± 31[a]	118 ± 31[a]
pCOD (mg/L)	92 ± 43[a]	92 ± 43[c]	66 ± 40[bc]	31 ± 16[ab]	80 ± 14	63 ± 25[a]
cCOD (mg/L)	59 ± 19[a]	59 ± 19	53 ± 17[b]	11 ± 7[ab]	8.3 ± 5[ab]	6 ± 5[ab]
sCOD (mg/L)	20 ± 16[a]	20 ± 16	24 ± 14[b]	38 ± 8[ab]	39 ± 19	51 ± 12[ab]
COD mass balance						
COD Effluent (Non-biomass) (% $tCOD_{in}$)	28 ± 13[a]	29 ± 37[c]	22 ± 9[abc]	29 ± 8[ab]	19 ± 6[ab]	22 ± 5[ab]
COD redirection (% $tCOD_{in}$)	46 ± 15[a]	45 ± 60[c]	60 ± 10[abc]	50 ± 16[ab]	63 ± 10[ab]	48 ± 8[ab]
COD oxidation (% $tCOD_{in}$)	26 ± 14[a]	26 ± 14[c]	18 ± 10[abc]	21 ± 15[ab]	18 ± 10[ab]	30 ± 11[ab]
COD Capture efficiency (%)	24 ± 27[a]	79 ± 15[c]	69 ± 12[c]	62 ± 19[a]	55 ± 8[a]	45 ± 15[a]
tCOD removal efficiency (%)	66 ± 20[a]	65 ± 22[c]	59 ± 17[bc]	51 ± 8[ab]	47 ± 10[a]	51 ± 12[a]

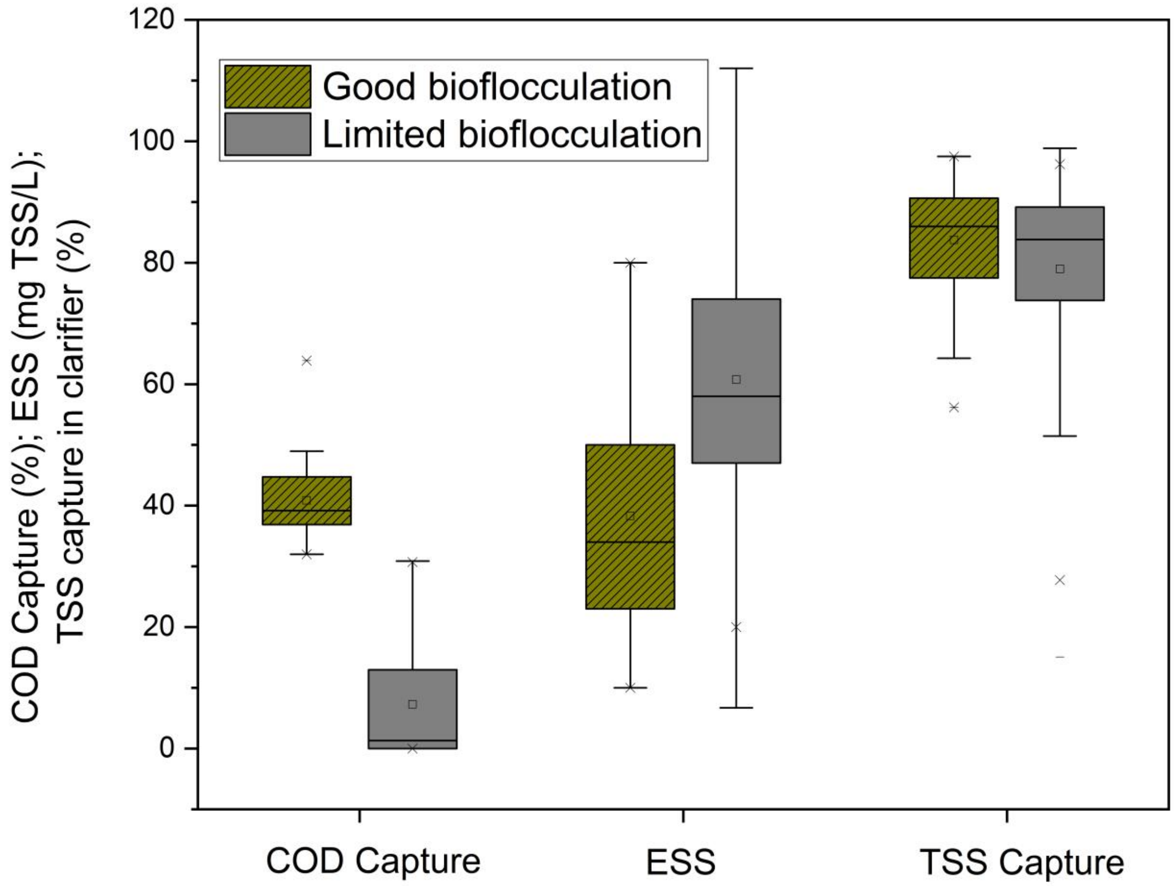

Figure 1: Average COD capture, effluent suspended solids (ESS) and TSS capture over the clarifier for the good and limited bioflocculation data set during scenario A (OUR-based wasting control without bioflocculation boundaries). Good and limited bioflocculation was defined by a statistical difference in effluent quality ($p < 0.05$) and TSS capture ($p < 0.1$) as carbon capture exceeded 31%.

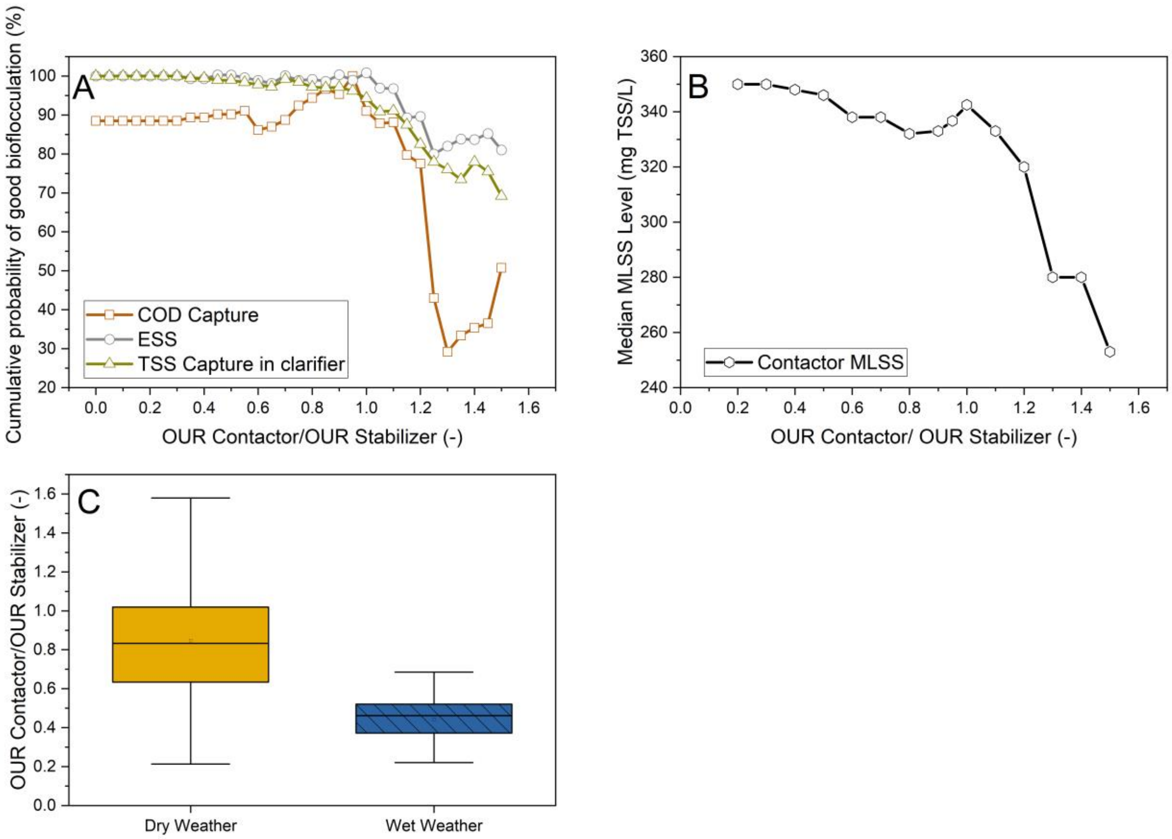

Figure 2: A: Probability (or chance) of achieving good bioflocculation criteria of COD capture > 31%, ESS < 48 mg TSS/L and TSS capture > 78% in function of minimum OUR ratio between contactor and stabilizer (Figure 1). B: Median MLSS levels in relation to a minimum OUR ratio level between contactor and stabilizer. C: OUR ratio for dry and wet weather events defined by plant influent flows to the full-scale WRRF below and above 1400602 m^3/d (370 MGD), respectively.

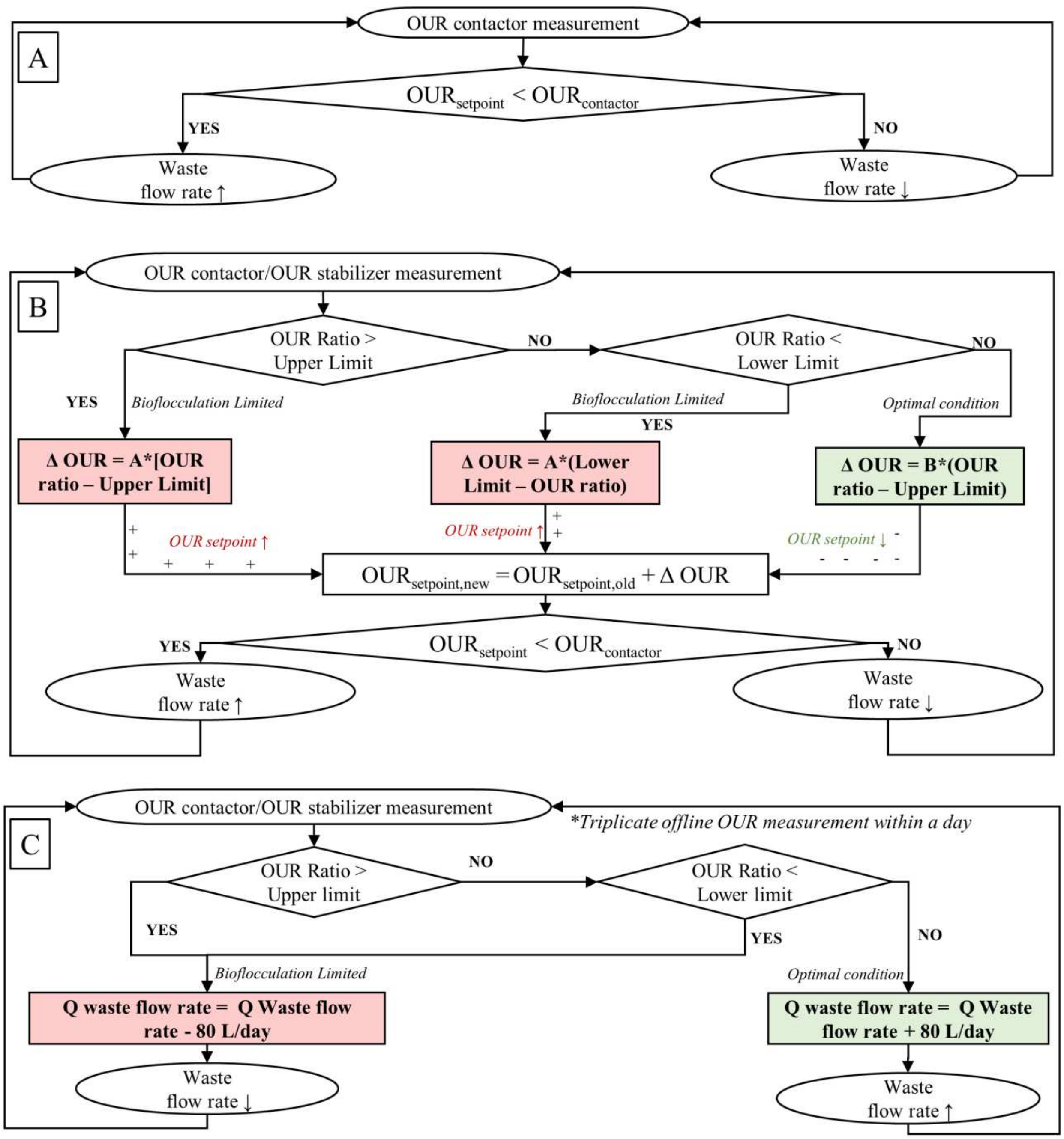

Figure 3: Scenario A was operated with OUR-based wasting control without bioflocculation boundaries (A) (Van Winkel, 2019; Van Winckel et al., in review). Bioflocculation boundaries were added into OUR-based wasting control (B) and wasting flow control (C). Scenario C applied a stepwise change in wasting setting rather than continuous changes as applied in scenario B. In addition, control decision were made within 20 minutes for scenario A and B, and on daily basis for scenario C.

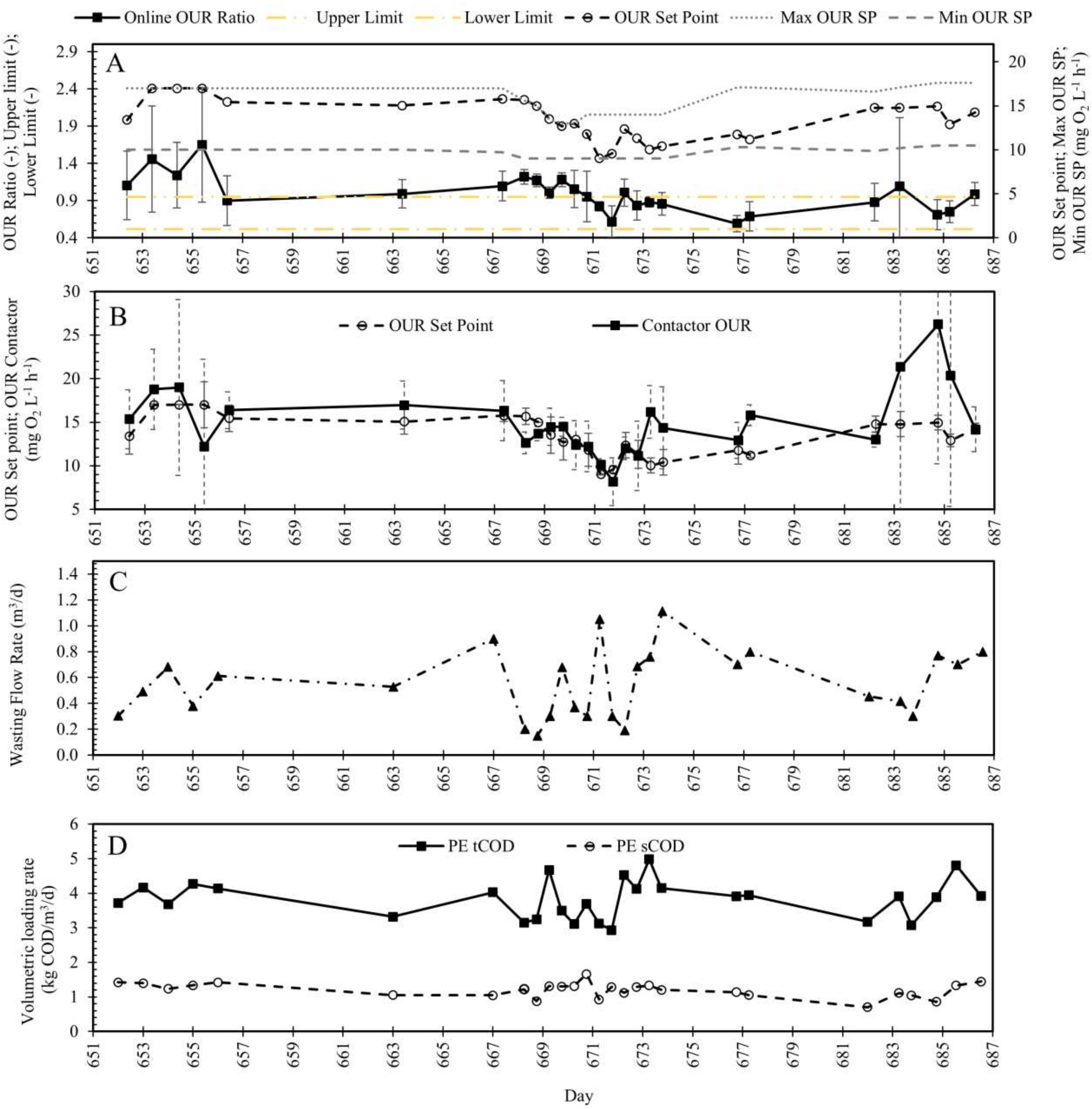

Figure 4: OUR ratio and OUR setpoint (A); OUR setpoint and contactor OUR (B); wasting flow rate (C) and the change of volumetric loading rate (D) as a result of applying the OUR wasting control logic with bioflocculation boundaries (see panel A), referred to as scenario B1 in Table 1 and 2. Figure 3B shows more details on control logic.

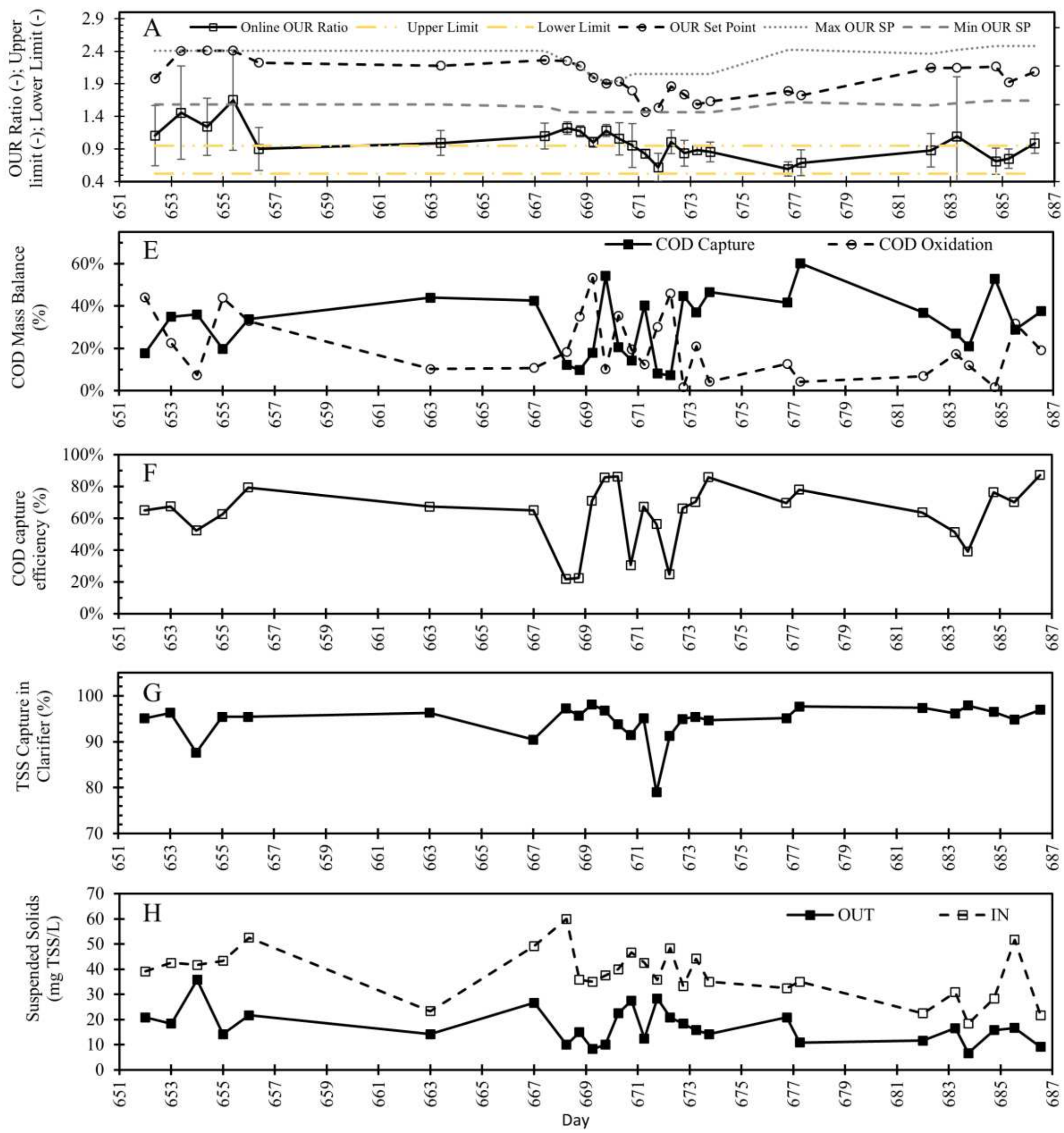

Figure 4 (continued): OUR ratio and OUR setpoint (A); carbon oxidation and capture (E); capture efficiency (F); TSS capture in clarifier (G), and effluent suspended solids (ESS) (H) as a result of applying the OUR wasting control logic with bioflocculation boundaries, referred to as scenario B1 in Table 1 and 2. Figure 3B shows more detail on control logic.

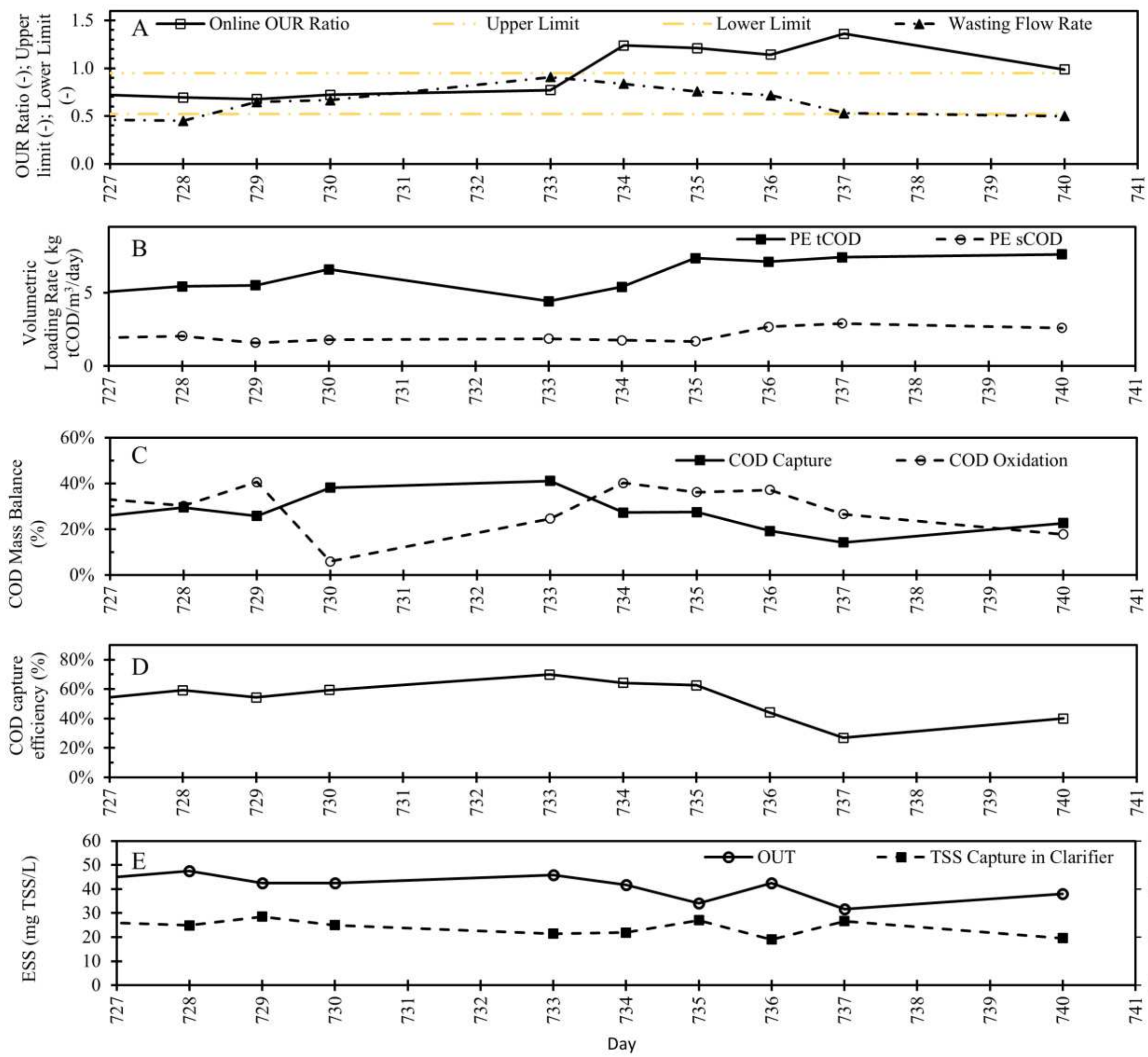

Figure 5: Wasting flowrate manipulated by OUR ratio (A); volumetric sCOD and tCOD loading (B); carbon oxidation and carbon capture (C); capture efficiency (D); effluent suspended solids (ESS), and TSS capture in clarifier (E) as a result of applying the flow waste control logic with bioflocculation boundaries, referred to as scenario C in Table 1 and 2. Figure 3B shows more detail on control logic.

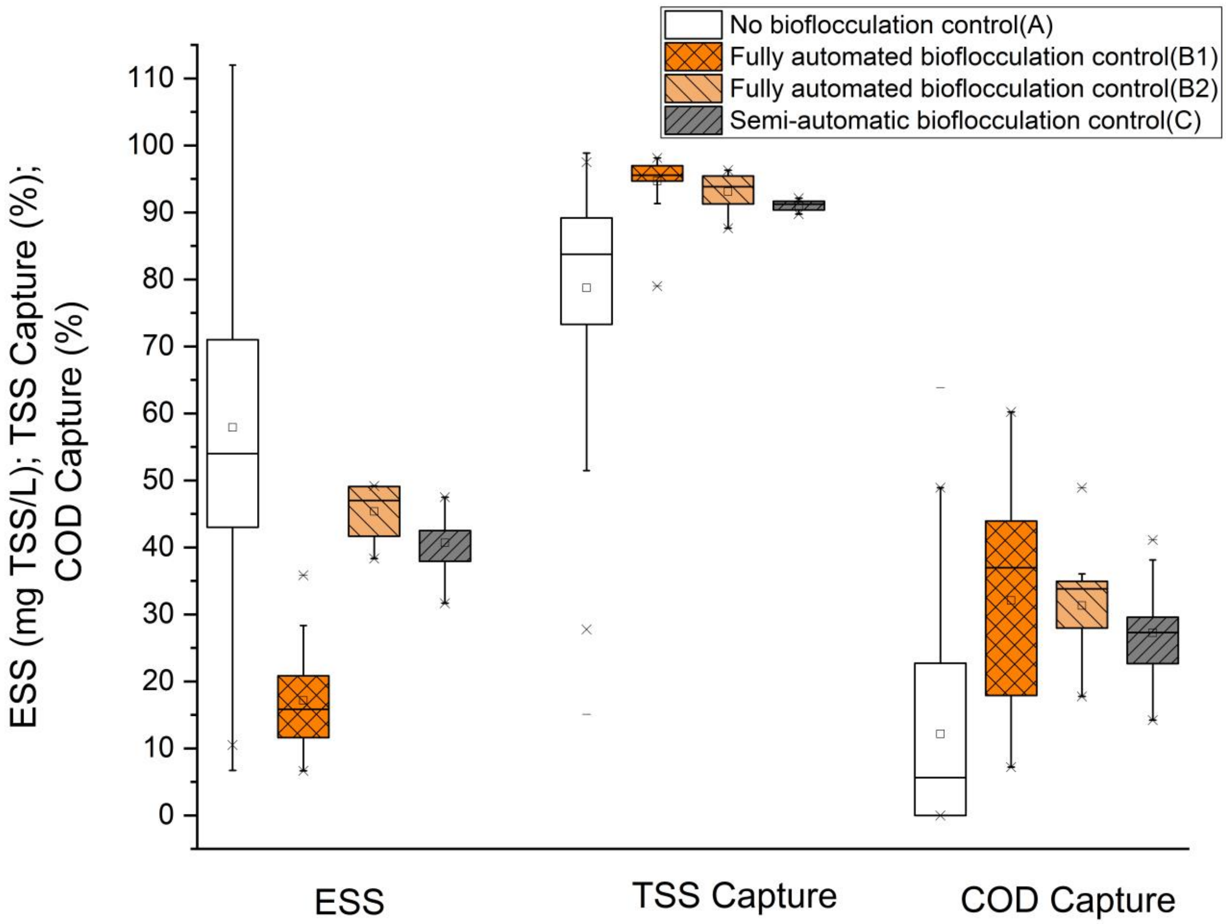

Figure 6: Summaries of all the bioflocculation criteria, including ESS, TSS capture, and COD capture for all control scenarios without bioflocculation boundaries (scenario A) and with bioflocculation boundaries (scenario B1, B2, and C). Figure 3 shows the details of the control logic and Table 1 and 2 show wastewater and operational conditions.

Supplemental Information

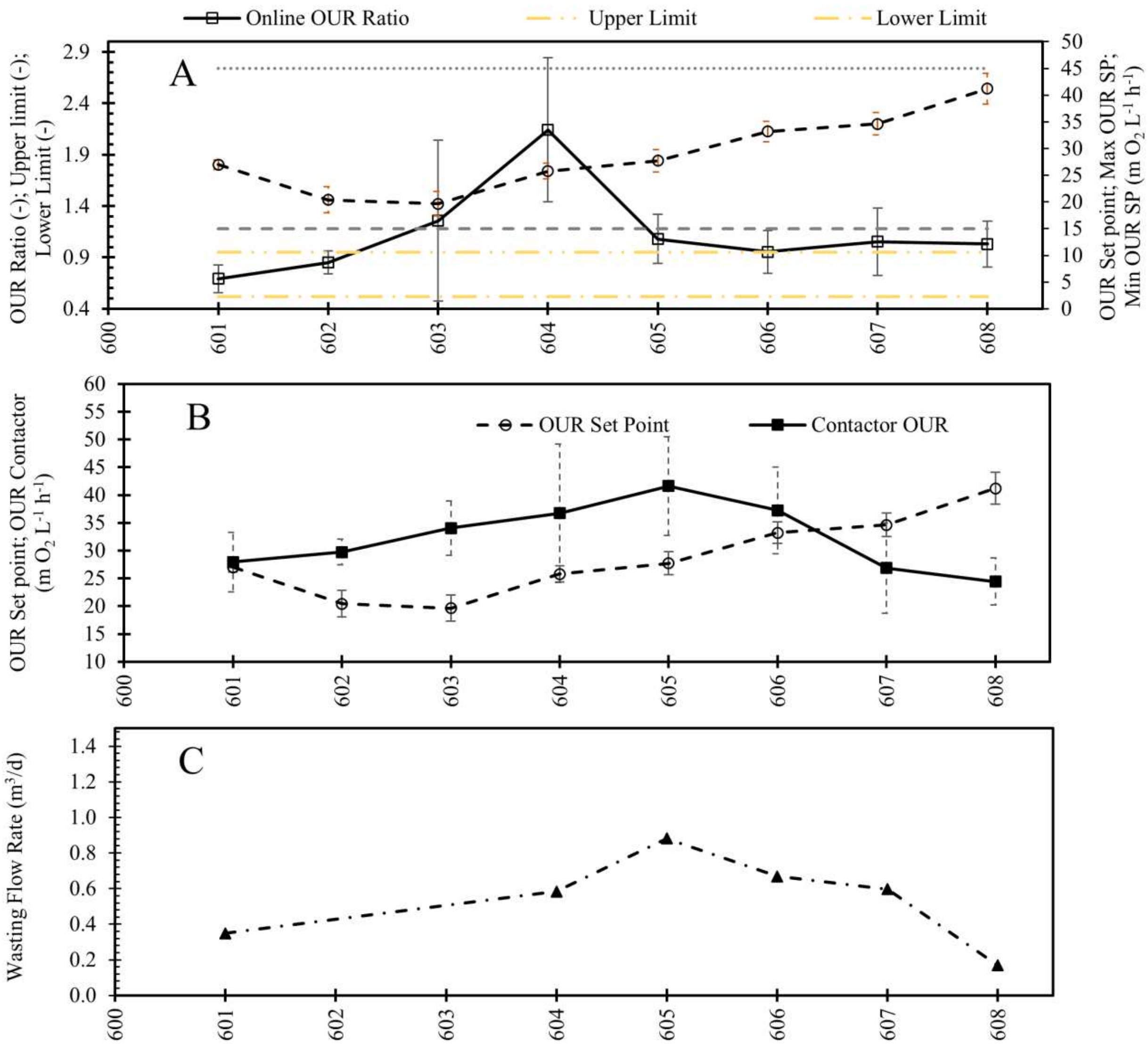

Figure S1: A proof of principle of scenario B2 with dynamic OUR-based wasting control with bioflocculation boundaries (Figure 3B) includes: OUR setpoint driven by OUR ratio (A); OUR setpoint and contactor OUR (B); and wasting flow rate (C).

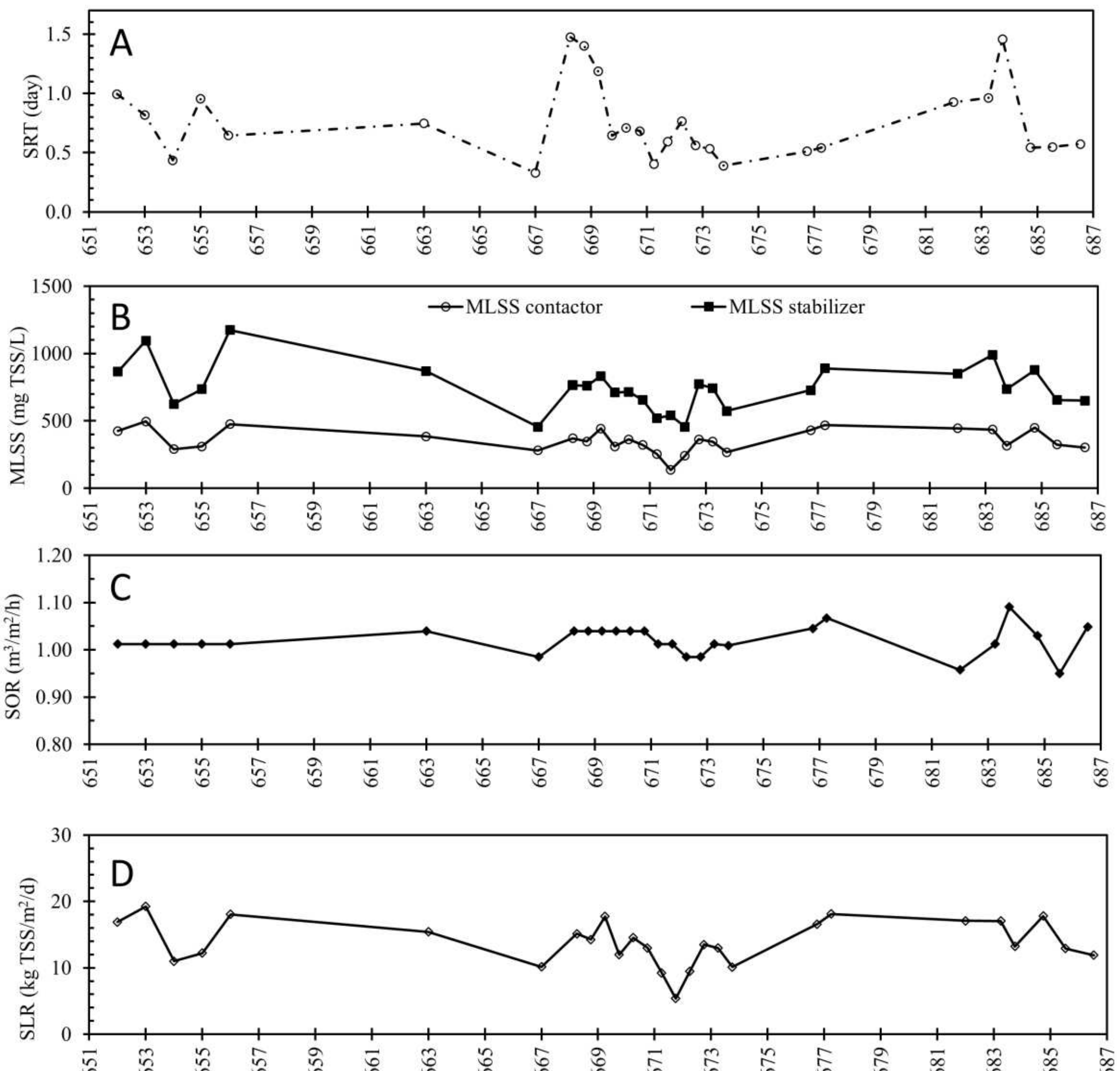

Figure S2: Operational conditions of scenario B1 consist of sludge retention time corrected at 20^{0}C (SRT); contactor and stabilizer TSS (B); surface overflow rate (SOR) (C); and sludge loading rate (SLR) (D).

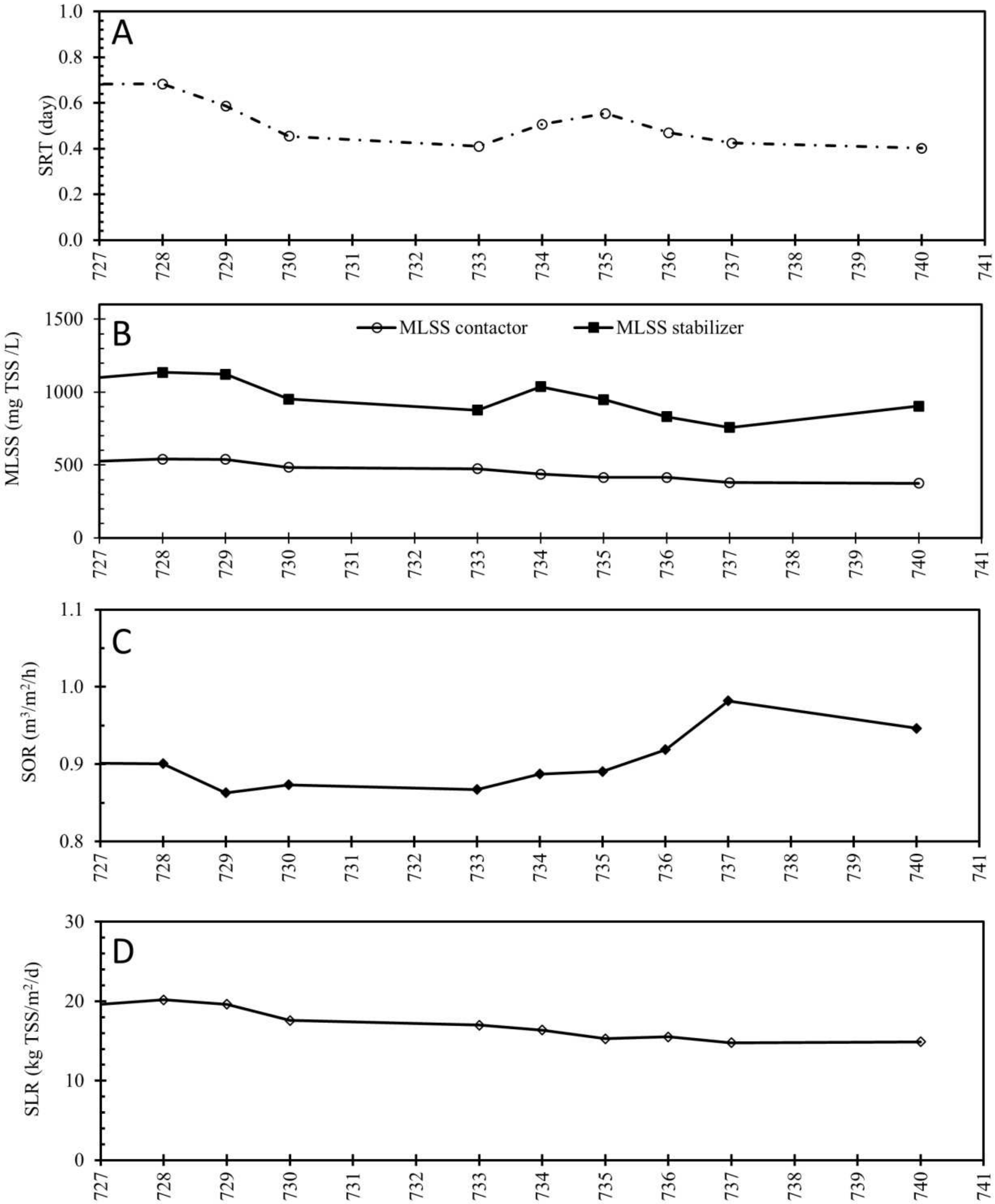

Figure S3: Operational conditions of scenario C consist of sludge retention time corrected at 20^0C (SRT); contactor and stabilizer TSS (B); surface overflow rate (SOR) (C); and sludge loading rate (SLR) (D).

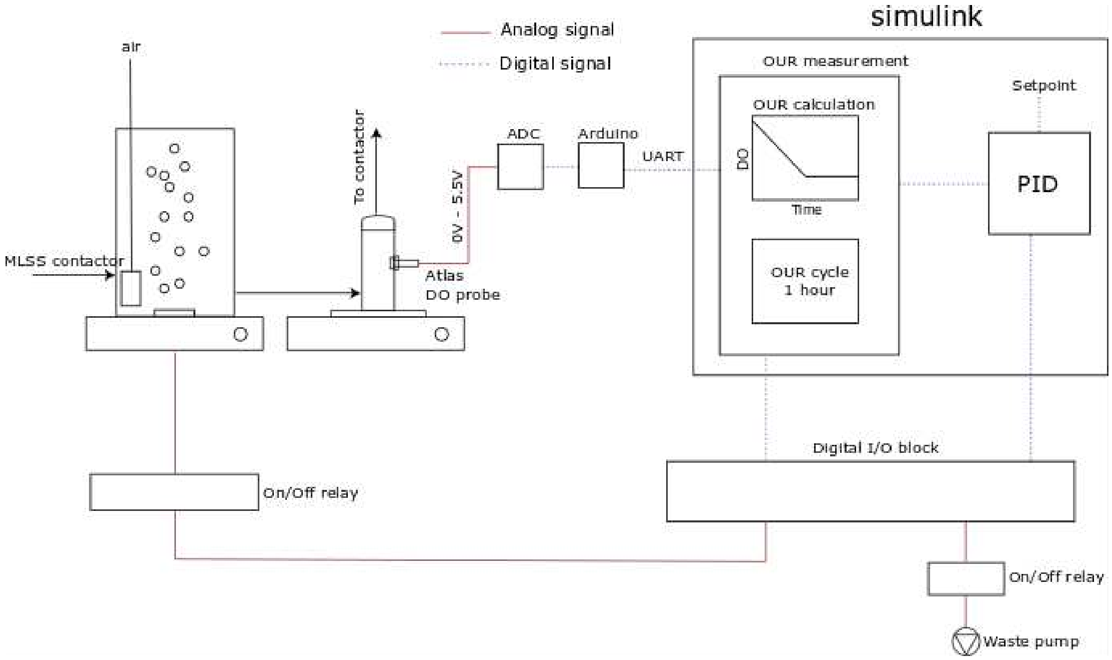

Figure S4. Simplified experimental setup for the automated on-line measurement of OUR. Solid lines indicate analog signals, while dotted lines represent digital signals (Figure is adapted from Van Winkel et al. 2019).

$$\%COD_{redirection} = \frac{M_{COD_{particulate\,wasted}} + M_{COD_{particulate\,effluent}}}{M_{COD_{influent}}} \quad (1)$$

$$\%COD_{capture} = \frac{M_{COD_{particulate\,wasted}}}{M_{COD_{influent}}} \quad (2)$$

$$\%COD_{particule\,effluent} = \frac{M_{COD_{particulate\,effluent}}}{M_{COD_{influent}}} \quad (3)$$

$$\%COD_{non\,biomass\,effluent} = \frac{M_{COD_{soluble\,effluent}} + M_{COD\,colloidal\,effluent}}{M_{COD_{influent}}} \quad (4)$$

$$\%COD_{oxidation} = 100 - \%COD_{redirection} - \%COD_{non\,biomass\,effluent} \quad (5)$$

Supplemental information S5: Calculation details of COD mass balances over high-rate system. The approach was similar to Rahman et al. (2016).